Optimal Design of Multiple Q-shells experiments for Diffusion MRI

Emmanuel Caruyer, Jian Cheng, Christophe Lenglet, Guillermo Sapiro, Tianzi Jiang, Rachid Deriche

HAL Id: inria-00617663

https://hal.inria.fr/inria-00617663

Submitted on 30 Aug 2011

Optimal Design of Multiple Q-shells experiments for Diffusion MRI

Emmanuel Caruyer[1], Jian Cheng[1,2], Christophe Lenglet[3], Guillermo Sapiro[4], Tianzi Jiang[2], Rachid Deriche[1]

[1] Athena Project-Team, Inria Sophia Antipolis - Méditerranée, France.
[2] Center for Computational Medicine, LIAMA, Institute of Automation, Chinese Academy of Sciences, China.
[3] Center for Magnetic Resonance Research, U of Minnesota Medical School, USA.
[4] Department of Electrical and Computer Engineering, U of Minnesota, USA.
Emmanuel.Caruyer@inria.fr

Abstract. Recent advances in diffusion MRI make use of the diffusion signal sampled on the whole Q-space, rather than on a single sphere. While much effort has been done to design uniform sampling schemes for single shell experiment, it is yet not clear how to build a strategy to sample the diffusion signal in the whole Fourier domain. In this article, we propose a method to generate acquisition schemes for multiple Q-shells experiment in diffusion MRI. The acquisition protocols we design are incremental, which means they remain approximately optimal when truncated before the acquisition is complete. Our method is fast, incremental, and we can generate diffusion gradients schemes for any number of acquisitions, any number of shells, and any number of points per shell. The samples arranged on different shells do not share the same directions. The method is tested for Spherical Polar Fourier reconstruction of the diffusion signal, and based on Monte-Carlo simulations, several preferred acquisition parameters are identified.

1 Introduction

Diffusion MRI maps the intravoxel diffusion characteristics of water molecules, in order to infer properties on the underlying tissue microstructure. The MR signal attenuation, $E(\mathbf{q})$, is related to the diffusion Ensemble Average Propagator (EAP), $P(\mathbf{r})$, through a Fourier transform. The diffusion tensor model [4] is based on the assumption of multivariate Gaussian probability to model the EAP. It is to date the most popular technique for clinical applications, because it is described by only 6 parameters, and can be reconstructed from a small number of diffusion weighted images. Unfortunately it is unable to describe complex tissue microstructure such as fiber bundle crossing in brain white matter. To overcome the shortcomings of Gaussian assumption, several high angular resolution diffusion imaging techniques are used, such as Q-ball imaging [18], to map the orientation distribution function. Recently, emerging reconstruction methods have been proposed [12, 1, 13, 2, 9] to make use of the diffusion signal in the

whole Fourier space, instead of on a unique sphere. These techniques require intensive sampling in the q-space to reconstruct $E(q)$, and the design of a sampling strategy is crucial for the development of such methods,

Single shell experiment design have received much attention from the diffusion MRI community [15, 14, 11, 16]. However we are aware of only one study [3] on multiple shells acquisition design; yet it does not explicitly provide a method to design acquisition protocols. In this context, we present in this paper a method to design multiple shells sampling schemes. Similarly to what has been proposed for single q-shell experiment design [6, 10, 8], our sampling is incremental, so as to be able to make use of corrupted data or aborted scans. Our method is tested using Monte-Carlo simulations on several synthetic diffusion models, for the reconstruction of the diffusion signal in the Spherical Polar Fourier (SPF) basis, which was recently introduced to represent the 3D diffusion signal [3].

2   Method

We first present a method to design sampling protocols on several spheres in q-space. The number of shells and the number of points per shell can be set to any desired value. Then we review the SPF reconstruction technique ([3, 5]), and present 4 synthetic diffusion models used in the next section for validation.

2.1   Multiple Shells experiment design

In this section, we propose a method to arrange a set of M points, on a set of K spheres of given radii q_k in $\mathbb{R}^3$. The method can generate any the number of points M and spheres K, with the desired radius q_k and number of points $N(q_k)$ for each shell.

Electrostatic repulsion In single q-shell experiment design, the problem is to uniformly distribute points on a sphere, keeping in mind that the signal is antipodally symmetric, hence $\mathbf{q}$ and $-\mathbf{q}$ play the same role. The solution proposed in [11] is to minimize:

$$J = \sum_{i \neq j} e(\mathbf{q}_i, \mathbf{q}_j), \text{where } e(\mathbf{q}_i, \mathbf{q}_j) = \frac{1}{|\mathbf{q}_i/q_i - \mathbf{q}_j/q_j|} + \frac{1}{|\mathbf{q}_i/q_i + \mathbf{q}_j/q_j|}. \quad (1)$$

We propose a generalization of this electrostatic repulsion for multiple shells: $E = (1 - \lambda)E_1 + \lambda E_2$, where $E_1 = \sum_k \omega_k J_k$ is the weighted sum of the electrostatic repulsion J_k on each shell of radius q_k, and $E_2 = \sum_{i \neq j} e(\mathbf{q}_i, \mathbf{q}_j)$ is a coupling term between shells.

The first term E_1 guarantees a uniform coverage of each single shell, while E_2 ensures that the global angular coverage is also approximately uniform. Note that for $\lambda = 0$, the minimization of E would be underconstrained, as any rotation of a shell with respect to the other does not modify the energy E_1. In order for the number of points on shell k to be proportional to $N(q_k)$ (where the choice of the function N is driven by the diffusion problem), it can be shown that taking the weights should be chosen as $\omega_k = 1/N(q_k)$.

Incremental construction of an optimal arrangement Some recent work on single shell acquisition design [6, 10, 8] are about the interest of incremental sampling sequences, for which an interruption at any point would result in an approximately optimal design. Such designs are useful to process data from prematurely aborted acquisitions, as well as to process data online. In the sequel we adapt the approach proposed in [8] to the problem of multiple q-shells design. To find a nearly optimal design for M points, M iterations are required. At each iteration i, we find the point $\mathbf{q}_i$ minimizing E, while the $\mathbf{q}_j, j < i$ remain fixed. The minimization is done by an exhaustive search among a set of 10000 pseudo-random points uniformly distributed on each sphere. As shown in the results section, this method provides a good approximation of the solution, with a huge gain in efficiency.

2.2 Synthetic data and reconstruction

The reconstruction with our experiment designs are tested for different diffusion models: one fiber (Gaussian diffusion), 2 fibers (mixture of Gaussian) with a 90° and a 60° crossing angle. Beyond these classical models, we also tested on a restricted diffusion model within a cylinder, for which the diffusion signal was computed according to [17], to test different radial behaviour. For the Gaussian models, the diffusion tensor was chosen with eigenvalues $\lambda_1 = 1.7 \text{mm}^2.\text{s}^{-1}$, and $\lambda_2 = \lambda_3 = 0.2 \text{mm}^2.\text{s}^{-1}$. The cylinder dimensions are $L = 5\text{mm}$ and $\rho = 5\mu\text{m}$.
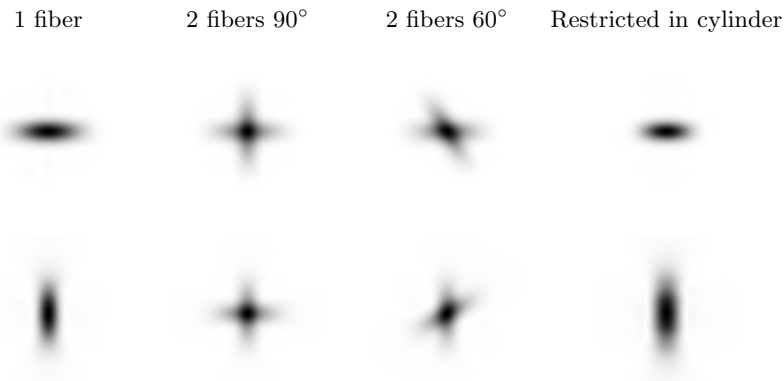
| 1 fiber | 2 fibers 90° | 2 fibers 60° | Restricted in cylinder |

Fig. 1. Diffusion signal (top) and diffusion propagator (bottom) for the 4 models selected for synthetic data generation. They are displayed in the x, y-plane.

The diffusion signal $E(\mathbf{q})$ is reconstructed in the spherical polar Fourier (SPF) basis $\{B_{nlm}; n \leq N, l \leq L, |m| \leq l\}$, recently introduced in [3]. The functions are defined as $B_{nlm}(q\,\mathbf{u}) = \kappa_n(\zeta) \exp(-q^2/2\zeta) L_n^{1/2}(q^2/\zeta) Y_{lm}(\mathbf{u})$, where κ_n

is a constant, Y_{lm} is the modified spherical harmonic basis for real and symmetric functions, and $L_n^{1/2}$ is the generalized Laguerre polynomial. It can represent the diffusion signal in the whole 3D space, using few coefficients [3]. Besides, a method called SPF imaging [5] was recently introduced to represent the EAP in a dual basis, with the same coefficients a_{nlm}. In our experiments, the SPF basis was truncated at radial and angular orders $N = 3$ and $L = 4$ respectively, as suggested in [3,5], which corresponds to 60 coefficients to estimate. The reconstruction error we computed to evaluate the accuracy of the reconstruction $\hat{a}_{nlm}$ is the relative root mean squared error (RMSE) to the ground truth:

$$\text{RMSE} = \sqrt{\frac{\sum_{nlm} |\tilde{a}_{nlm} - \hat{a}_{nlm}|^2}{\sum |\tilde{a}_{nlm}|^2}} \tag{2}$$

and the ground truth coefficients $\tilde{a}_{nlm}$ are estimated from 10000 samples uniformly distributed in the q-space.

3 Results

The minimization of E with respect to $\{\mathbf{q}_i, i = 1 \ldots M\}$ was implemented. In the sequel we present the sampling schemes generated, and evaluate them for diffusion MRI measurement.

3.1 Multiple shells experiment design

We have constructed incremental point sets minimizing the energy E. We plot in Fig. 2 the results for a number of points on shell k proportional to $N(q_k) = q_k^2$, which corresponds to a uniform arrangement of points. The construction of a set of $M = 120$ points took 4s on a laptop with a 2.8GHz Intel® Core™ 2 Duo processor and 4GB memory, with a python implementation. An optimal arrangement of 120 points on 3 q-shells is presented in Fig. 2, for $N(q) = q^2$ and $\lambda = 0.1$. The angular density of each shell is approximately optimal, as well as the global angular coverage.

The electrostatic energy J_k is calculated for each shell, and normalized to the minimum energy, of the optimal arrangement (as provided with the Camino toolkit [7]). As reported in Fig. 2, it remains very close to 1; this means that the electrostatic energy of our approximate optimum is very close to the global minimum. We also check the minimum angle between any two points, which is a metric used to check the uniformity of a sample distribution [14]. As expected, the approximate solution contains slightly closer points than the optimal solution, but both remain within the same range.

3.2 Reconstruction in SPF basis

Because there is a large number of degrees of freedom in q-space experiment design, we organize our investigations as follows. First, for a given number of
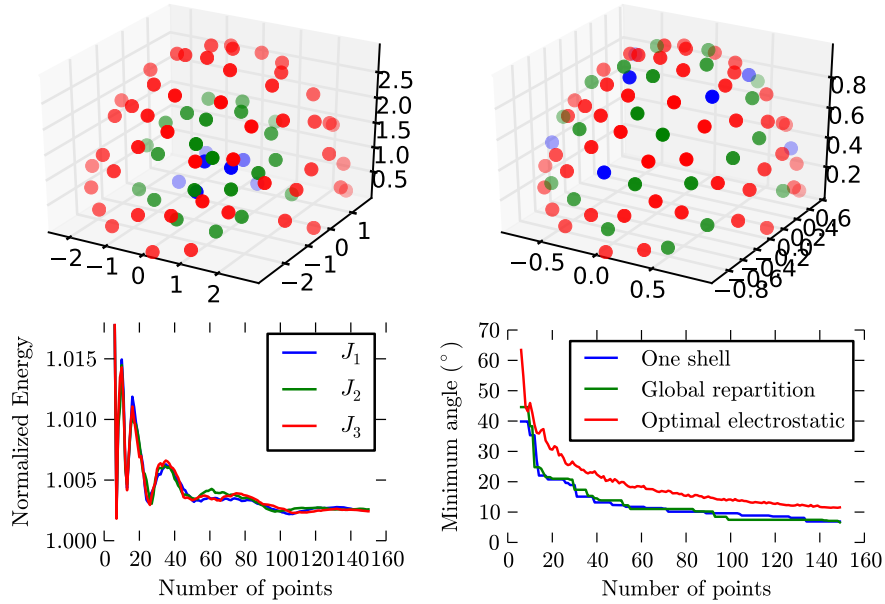
Fig. 2. (top left) Multiple q-shell experiment design: 120 points on 3 shells, with $N(q) = q^2$. (top right) Points reprojected on the unit sphere. The distribution of points on each shell is uniform, as well as the global angular density. (bottom left) Normalized electrostatic energy. (bottom right) Minimum angle between any two points.

samples and a given number of shells, we analyze how to best distribute the points between shells (choice of the function $N(q_k)$). Then we evaluate the influence of the number of shells K on the reconstruction. Finally, we evaluate the influence of the correlation of sampling directions between shells. The proposed acquisition strategies are tested without noise, and in presence of Rician noise in the measurements. Unless explicitly modified, the SNR was set to 30 for all experiments. The shells radii are distributed linearly between q_{min} and $q_{max} = \sqrt{b_{max}/4\pi^2\tau}$, with a maximum b-value $b_{max} = 5\,000\text{s} \cdot \text{mm}^{-2}$ and a diffusion time $\tau = 20.8\text{ms}$. The reconstruction in SPF basis is a regularized least squares estimation of the coefficients [3, 5], and the radial and angular regularization weights are $\lambda_n = \lambda_l = 10^{-8}$.

Number of points per shell With no prior knowledge on the signal characteristics, the intuition would be to arrange the samples uniformly in the q-space, thus choosing a number of points $N(q_i)$ on the i-th shell proportional to q_i^2. However, it is known that the radial behaviour of the signal is Gaussian-like, which means that the energy is concentrated near the origin. So it might be that $N(q_i) = q_i^2$ is not the best sampling strategy.
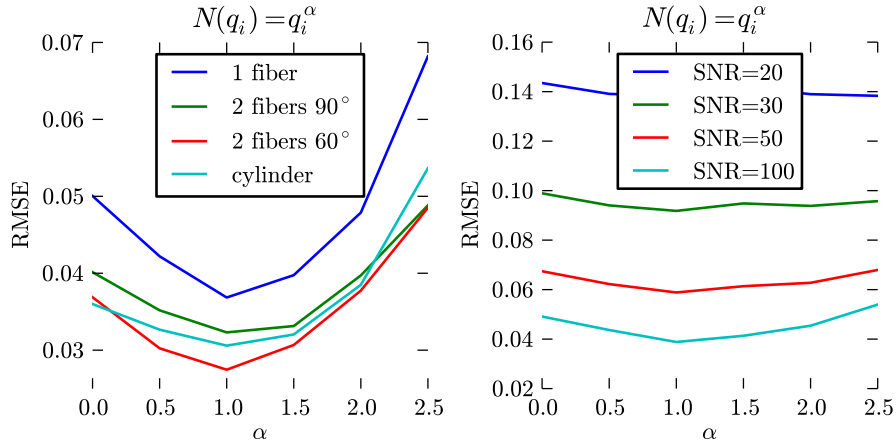
Fig. 3. Effect of the number of points per shell $N(q_i)$ on the reconstruction accuracy. The number of measurements was set to 120, constrained on 3 q-shells, with q_1, q_2, q_3 linearly arranged. (left) no noise, (right) various SNR values, for the 2 fibers 90° model

Interestingly, the results in Fig. 3 suggest that a number of points on shell i proportional to q_i gives best results. This corresponds to weighting the natural solution $N(q_i) = q_i^2$ by a factor $1/q_i$, giving more importance to the measurements at low q. This result is shared by the 4 diffusion models of interest, as well as for a wide range of SNRs.

Number of shells The effect of changing the number of shells is investigated, for various diffusion models and total number of points (Fig. 4). It is clear that 3 shells give the best reconstruction, whatever the diffusion model or the number of measurements. When one changes the radial truncation order N of the SPF basis, the optimal number of shells changes accordingly (results not reported here).

Coherence between shells The second term E_2 in the repulsion energy we propose in 2.1 tends to separate the point directions from one shell to another. As a means of comparison, we designed a sampling scheme with the same number of points per shell, but with coherent directions (see Fig. 5). Choosing incoherent directions between shells allows a better reconstruction in SPF basis. The difference increases with the number of shells: for the coherent directions strategy, the total number of separate directions decreases, while it remains stable for the incoherent shells acquisition design.
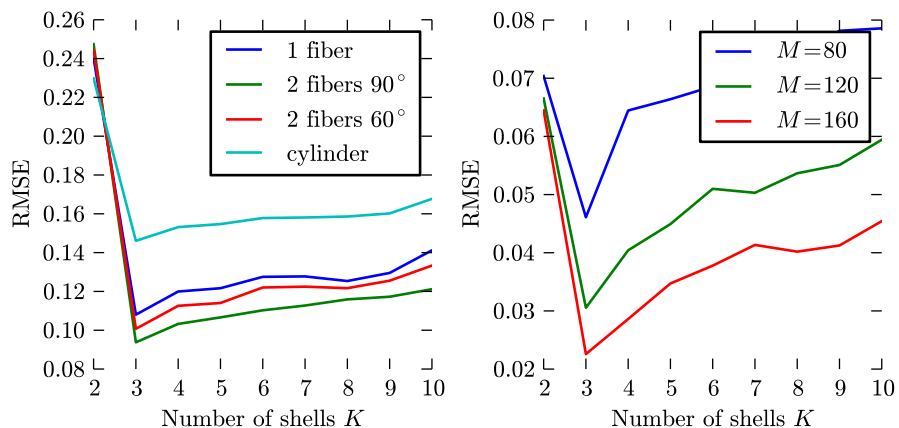
Fig. 4. Effect of the number of shells on the reconstruction, for various diffusion models (left) and total number of measurements M (right)

4   Discussion and conclusion

In this article, we have proposed an original approach to the design of sampling schemes for multiple q-shells acquisition. The method is fast, and can provide sampling schemes, with any arrangement for which the number of points on shell k is proportional to an arbitrary function $N(q_k)$. Different sampling strategies were tested for the reconstruction of SPF coefficients. A remarkable result is the advantage of using separate diffusion directions between shells, instead of reusing the same directions. Also, the optimal number of shells seems to be equal to 3, for the reconstruction in the SPF basis truncated at radial order 3.

Acknowledgments

References

1. Aganj, I., Lenglet, C., Sapiro, G., Yacoub, E., Ugurbil, K., Harel, N.: Reconstruction of the orientation distribution function in single and multiple shell q-ball imaging within constant solid angle. Magn. Reson. Med. (2009), in press
2. Assemlal, H.E., Tschumperlé, D., Brun, L.: Evaluation of q-space sampling strategies for the diffusion magnetic resonance imaging. In: MICCAI. London, England (September 2009)
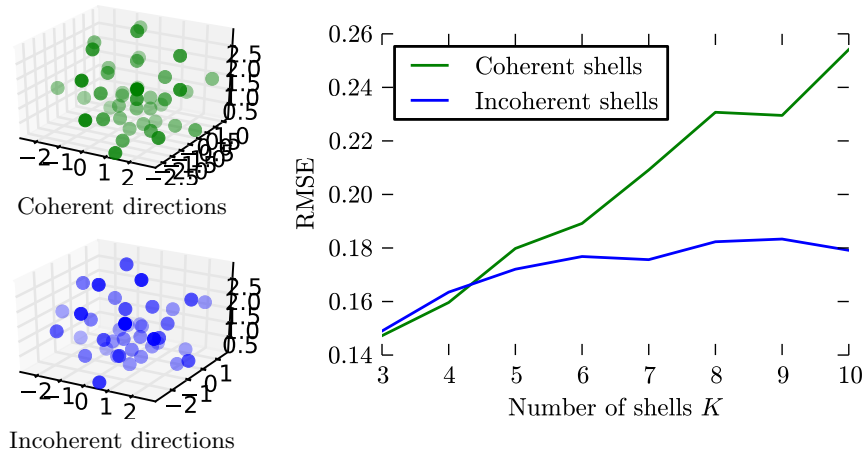
Fig. 5. (left) example of coherent and incoherent directions. (right) Consequence on the reconstruction, for a total of $M=60$ measurements.

3. Assemlal, H.E., Tschumperlé, D., Brun, L.: Efficient computation of pdf-based characteristics from diffusion mr signal. In: MICCAI. pp. 70–78. Springer-Verlag, Berlin, Heidelberg (2008)

4. Basser, P.J., Mattiello, J., Lebihan, D.: MR Diffusion Tensor Spectroscopy and Imaging. Biophysical Journal 66, 259–267 (1994)

5. Cheng, J., Ghosh, A., Jiang, T., Deriche, R.: Model-free and Analytical EAP Reconstruction via Spherical Polar Fourier Diffusion MRI. In: MICCAI. Beijing, China (2010)

6. Cook, P.A., Symms, M., Boulby, P.A., Alexander, D.C.: Optimal acquisition orders of diffusion-weighted mri measurements. J Magn Reson Imaging 5(25), 1051–8 (May 2007)

7. Cook, P. A. anb Bai, Y., Nedjati-Gilani, S., Seunarine, K.K., Hall, M.G., Parker, G.J., Alexander, D.C.: Camino: Open-source diffusion-mri reconstruction and processing. In: 14th ISMRM. Seattle, USA (May 2006)

8. Deriche, R., Calder, J., Descoteaux, M.: Optimal real-time q-ball imaging using regularized Kalman filtering with incremental orientation sets. Med. Image Anal. 13(4), 564–579 (August 2009)

9. Descôteaux, M., Deriche, R., LeBihan, D., Mangin, J.F., Poupon, C.: Diffusion propagator imaging: Using laplace's equation and multiple shell acquisitions to reconstruct the diffusion propagator. In: IPMI. p. 1–13. LNCS 5636 (2009)

10. Dubois, J., Poupon, C., Lethimonnier, F., Le Bihan, D.: Optimized diffusion gradient orientation schemes for corrupted clinical DTI data sets. MAGMA 19(3), 134–43 (2006)

11. Jones, D.K., Horsfield, M.A., Simmons, A.: Optimal strategies for measuring diffusion in anisotropic systems by magnetic resonance imaging. Magn. Reson. Med. 42(3), 515–525 (September 1999)

12. Khachaturian, M.H., Wisco, J.J., Tuch, D.S.: Boosting the sampling efficiency of QBI using multiple wavevector fusion. Magn Reson Med 57(2), 289–296 (2007)

13. Ozarslan, E., Koay, C.G., Shepherd, T.M., Blackband, S. J. andBasser, P.J.: Simple harmonic oscillator based reconstruction and estimation for three-dimensional q-space mri. In: 17th ISMRM. Hawai, USA (April 2009)
14. Papadakis, N.G., Murrills, C.D., Hall, L.D., Huang, C.L., Adrian Carpenter, T.: Minimal gradient encoding for robust estimation of diffusion anisotropy. Magn Reson Imaging 18(6), 671–9 (2000)
15. Papadakis, N.G., Xing, D., Huang, C.L.H., Hall, L.D., Carpenter, T.A.: A comparative study of acquisition schemes for diffusion tensor imaging using mri. Journal of Magnetic Resonance 137(1), 67–82 (March 1999)
16. Skare, S., Hedehus, M., Moseley, M.E., Li, T.Q.: Condition number as a measure of noise performance of diffusion tensor data acquisition schemes with mri. J Magn Reson 147(2), 340–352 (December 2000)
17. Soderman, O., Jonsson, B.: Restricted Diffusion in Cylindrical Geometry. Journal of Magnetic Resonance, Series A 117(1), 94–97 (nov 1995)
18. Tuch, D.S.: Q-ball imaging. Magn. Reson. Med. 52(6), 1358–1372 (2004)